The Role of Mass Transfer in the Removal of Heavy Metal Ions by Ion Exchange Using Batch Gas Sparged Vessel

T. M. Zewail
Chemical Engineering Department, Faculty of Engineering,
Alexandria University, Alexandria 21544, Egypt

Original scientific paper
Received: September 22, 2009
Accepted: May 19, 2010

Mass transfer behaviour of a batch gas sparged vessel for conducting ion exchange reactions involving heavy metal removal has been investigated. The effect of various parameters such as type of heavy metal ion (Ni^{2+}, Cd^{2+}), superficial gas velocity, physical properties of the solution and temperature on the mass transfer coefficient was studied. It has been found that mass transfer coefficient increases as gas superficial velocity and temperature increase. At equilibrium, a maximum removal efficiency of 99.98 % was obtained for Ni^{2+} and Cd^{2+}. Activation energy calculations gave the values of $E = 2.4$ and 3.3 kJ mol^{-1} for Ni^{2+} and Cd^{2+} respectively. These values confirm the diffusion controlled nature of ion exchange reactions. Dimensional analysis of the present mass transfer data led to the following correlations:

For Ni^{2+} $J_D = 0.334\ (\mathrm{Re} \cdot \mathrm{Fr})^{-0.14}$
For Cd^{2+} $J_D = 0.125\ (\mathrm{Re} \cdot \mathrm{Fr})^{-0.25}$

The importance of these mass transfer correlations in the design and operation of gas sparged vessels used for conducting ion exchange reaction was highlighted.

Key words:
Mass transfer, ion exchange, gas sparging, heavy metal removal

Introduction

Mass transfer plays an important role in many industrial processes such as electrochemical processes, biochemical reactions conducted on immobilized enzymes, membrane processes and heterogeneous (liquid-solid, gas-liquid and liquid-liquid) and catalytic reactions. Enhancement of mass transfer rate in such processes is an important task in industrial applications to increase the space time yield.

Methods used to enhance mass transport in such diffusion controlled reactions include mechanical stirring,[1] vibro-agitation,[2] the use of turbulence promoters[3–5] jet impingement[6,7] and gas sparging.[8–10] Gas sparging particularly is gaining wide acceptance as a means for enhancing mass transfer controlled reactions in view of the lower power consumption of gas sparging compared with mechanical stirring;[11] in addition gas sparging is simple and offers considerable advantages over mechanical stirring such as elimination of expensive moving parts which need regular maintenance.

The ion exchange process is a typical example of a liquid-solid diffusion controlled process, which is defined as a process in which mobile ions from an external solution are exchanged for ions that are electrostatically bound to the functional group contained within a solid matrix known as the ion exchanger or resin. When the functional groups are negatively charged, the exchange will involve cations, and when they are positively charge they involve anions. Ion exchange is a highly popular technology and has been widely practiced in many industrial applications such as pharmaceutical purification, water softening processes, wastewater treatment processes, separation and purification in the food industry and manufacture of ultrapure water used in semiconductor processes.[12] There are two mass transfer-resistances in ion exchange reactions. The first is the external mass-transfer resistance due to the film or boundary layer surrounding the ion-exchange particle. The second is the intra-particle diffusion resistance due to porosity (ion diffusion inside the resin particle). Either or both resistances can be the rate-controlling step.[13]

Although some work has been done on the rate of ion-exchange reactions under mechanical stirring conditions,[14,15] scant attention has been given to the use of gas sparging to enhance the rate of the ion-exchange process. The aim of the present work is to examine the effect of gas sparging on the rate of ion-exchange reactions for heavy metal ions removal from aqueous solution in relation to the following parameters: type of heavy metal (Ni^{2+}, Cd^{2+}), superficial gas velocity, temperature and

---

*Tel. + (203)5914475; Fax. + (203)5921853;
Email:tagchem04@yahoo.com

physical properties of the solution. In addition, a mass transfer correlation will be developed to quantify the process.

Two models have been presented in the literature to explain the effect of gas sparging on the rate of mass transfer, as follows:

(i) Natural convection model;[16,17] this model assumes that the buoyancy force arising from the density difference between the liquid and the gas-liquid dispersion gives rise to turbulent flow natural convection, the magnitude of which determines the rate of mass transfer at the solid surface. According to this model, dimensional analysis leads to:

$$Sh = a\ (Sc \cdot Ga)^{0.33}\ \varepsilon^{n} \qquad (1)$$

(ii) The surface renewal model,[18,19] which assumes that mass transfer takes place through a surface renewal mechanism based on the fact that the rising bubbles induce radial as well as axial momentum transfer by virtue of the ability of these bubbles to generate turbulence in their wakes. The surface renewal model correlates the mass transfer data in gas sparged system by the equation:

$$St \cdot Sc^{0.5} = 0.035\ (Re \cdot Fr)^{-0.25} \qquad (2)$$

Although these models explain qualitatively the mechanism by which mass transfer is enhanced in gas sparged system they cannot be used to predict the present data because of the simplifying assumptions involved in deriving eqs. (1) and (2) which are not always realistic. Therefore, the aim of the present study is to develop mass transfer equations that fit the present data.

Experimental

Fig. 1 shows the experimental setup used in the present work. It consisted mainly of a plexiglass cylindrical vessel, an air compressor and a calibrated rotameter. The cylindrical vessel was 14 cm in diameter and 30 cm in height. It was surrounded by a thermostated water bath to control the temperature of the vessel's contents. The base of the vessel was a sintered glass (G_2) gas distributor. Air at different flow rates was allowed to enter the vessel through the sintered glass gas distributor. The flow rate of inlet air was regulated by a ball valve and measured by a calibrated rotameter.

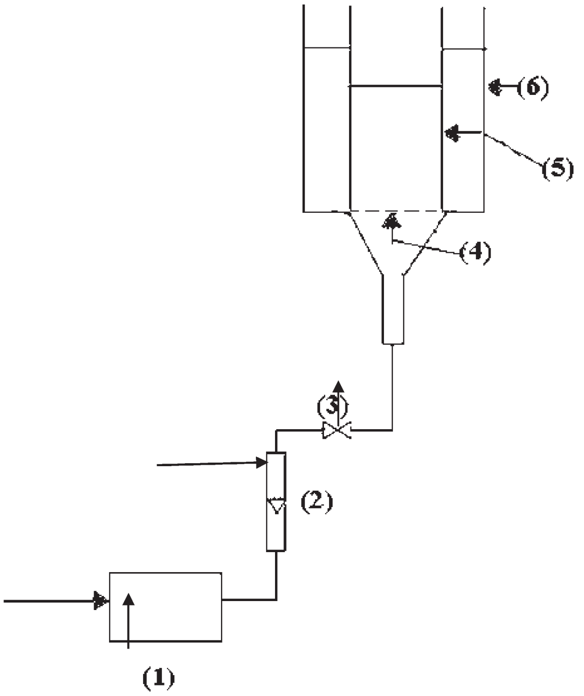

1 – air compressor, 2 – calibrated rotameter, 3 – ball valve, 4 – sintered glass distributor, 5 – plexiglass cylindrical container, 6 – thermostated water bath

Fig. 1 – *Experimental set up*

Nickel nitrate, cadmium chloride, hydrochloric acid, sodium hydroxide and glycerol used in solution preparations were all AR-grade chemicals. A strong cation exchange resin, macroporous monoplus SP112 (Bayer company) in hydrogen form was used in the present work. Prior to use, the resins were washed with 1 mol L^{-1} NaOH followed by 1 mol L^{-1} HCl, and finally with distilled water to remove grease and inorganic impurities. The properties of the ion exchange resin are given in Table 1. Freshly prepared solutions were used throughout all experiments. A stock solution of 1 kg m^{-3} of Ni^{2+}, Cd^{2+} was prepared using distilled water. The batch ion exchange experiments were carried out by plac-

Table 1 – *Properties of macroporous monoplus SP112 resin*

Data	Monoplus SP112
ionic form as shipped	H^{+}
functional group	sulphonic acid
matrix	crosslinked polystyrene
structure	macroporous
appearance	Beige-grey opaque
particle diameter, mm	0.73 ± 0.07
bulk mass, g L^{-1}	760
density, g mL^{-1}	1.18
total capacity, eql L^{-1}	1.6
max. operating temp., ° C	120
pH operating range	0–14

ing 2 L of freshly prepared solution of heavy metal ion (Ni^{2+}or Cd^{2+}) of known initial concentration in the vessel. Air-flow rate was adjusted at the required value by ball valve. The kinetics of the ion exchange reaction were monitored by withdrawing 5 mL sample from the vessel each 2–5 min; the samples were analyzed for the remaining heavy metal ion using atomic absorption. Physical properties of solutions were varied by adding glycerol of different percentages (5, 10, and 12.5 %). Density and viscosity of the solutions used were determined using a density bottle and an Ostwald viscometer[20] respectively. The diffusivities of Ni^{2+} and Cd^{2+} in solution were taken from literature.[21]

Results and discussion

Preliminary pH studies showed that maximum removal efficiency occurred in the pH range from 5 to 6 for Ni^{2+} and Cd^{2+} which are close to the pH of their solutions.

The mass transfer behavior of the present batch gas sparged vessel is based on the following differential material balance with respect to the ion to be removed:

$$-V_s \frac{d\gamma}{dt} = kA\gamma \tag{3}$$

This upon integration yields:

$$\ln \frac{\gamma_0}{\gamma} = \frac{kA}{V_s} \cdot t \tag{4}$$

Where γ_0, γ are initial and final concentrations of heavy metal ion respectively, V_s is the solution volume, t is the time, k mass transfer coefficient, A is the surface area of resin which has been calculated from the equation:

$$A = \frac{6m}{\bar{d}_s \rho_s} \tag{5}$$

Where m is resin mass, $\bar{d}$ is average resin particle diameter, ρ_s is resin density.

Figs. 2 and 3 show typical plot of ln (γ_0/γ) against time at different superficial gas velocities for Ni^{2+}, Cd^{2+} ions respectively. It is obvious that there are two different rate regimes, an initial rapid rate regime up to 10 min and slower rate regime from 10 to 40 min. This phenomenon may be attributed to the fact that ion exchange of Ni^{2+}, Cd^{2+} on resins takes place through two mechanisms:

(i) At the beginning, where the active sites are numerous, and the driving force is high, the only resistance to the rate of ion exchange is the liquid film diffusion layer surrounding each resin particle.

(ii) With increase of time, the driving force for mass transfer begins to decrease, while the number of available active sites on the resin becomes less and intra-particle diffusion becomes increasingly important. A similar approach was obtained by Amin *et al.*[22] who studied the rate of Cd^{2+} cementation on zinc using a rotating fixed bed reactor. The authors attributed this phenomenon to the presence of two different mechanisms namely, liquid phase diffusion and diffusion through a porous layer of the deposited metal.

The mass transfer coefficient k was determined at different superficial gas velocities from the slope of lines of the second regime since it is the rate-determining step. The effect of superficial gas velocity on the mass transfer coefficient at different Sc is shown in Figs. 4 and 5 for Ni^{2+}, Cd^{2+} respectively. Figs. 4 and 5 show that the mass transfer coefficient k increases with increasing superficial air velocity according to the following equations:

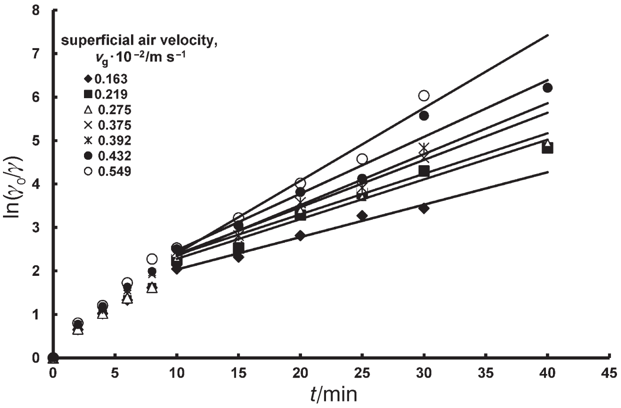

Fig. 2 – *Typical plot of ln γ_0/γ versus time at different superficial air velocities for the exchange of Ni^{2+}. (Initial Ni^{2+} concentration = 0.05 kg m^{-3}, resin mass, m = 0.02 kg, T = 298 K).*

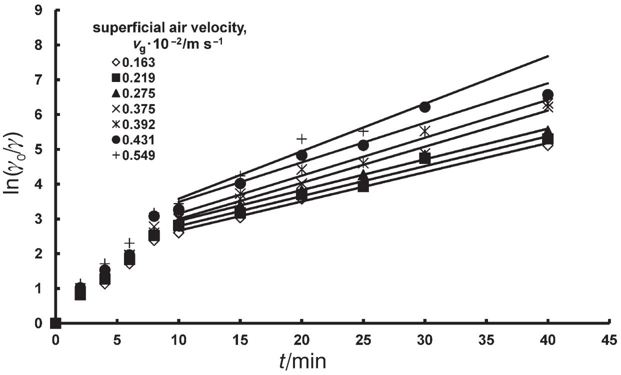

Fig. 3 – *Typical plot of ln γ_0/γ versus time at different superficial air velocities for the exchange of Cd^{2+}. (Initial Cd^{2+} concentration = 0.05 kg m^{-3}, resin mass, m = 0.02 kg, T = 298 K).*

For Ni^{2+}

$$k \,\alpha\, V_g^{0.58} \tag{6}$$

For Cd^{2+}

$$k \,\alpha\, V_g^{0.25} \tag{7}$$

The discrepancy between the mass transfer behaviour of Ni^{2+} and Cd^{2+} may be attributed to the tendency of Cd^{2+} to form complex compounds with Cl^- ions,[23] the formation of the chloro-complex reduces the concentration of free Cd^{2+} and the driving force for diffusion. Under such conditions, the rate of removal of Cd^{2+} by ion exchange is controlled not only by the liquid phase and intraparticle diffusion, but also by the degree of dissociation of the complex chloro Cd salt to simple Cd^{2+} ions. Such a complicating effect does not exist in the case of Ni^{2+}.

Increasing superficial air velocity enhances the rate of the ion exchange reaction by virtue of the ability of gas bubbles to induce radial as well as axial momentum, which reduces the film thickness around the resin particle.[24] Besides, as a result of the axial momentum generated by the rising gas bubbles, the ion exchange particle becomes fluidized with further enhancement in the rate of mass transfer by virtue of particle collision which disturbs the diffusion layer around each particle.

Figs. 4 and 5 show that the mass transfer coefficient decreases as Sc increases.

To correlate the present data using a dimensionless equation, the dimensionless groups J_D, Re and Fr usually used in correlating mass transfer data in gas sparged vessels, were used. Figs. 6 and 7 show that for the conditions $1325 < Sc < 2216$ and $3.8 \cdot 10^{-4} < Re \cdot Fr < 6.7 \cdot 10^{-3}$, the present mass transfer data for Ni^{2+} fit the equation:

$$J_D = 0.334\ (Re \cdot Fr)^{-0.14} \tag{8}$$

with an average deviation 4 %.

Figs. 8 and 9 show that for the conditions $747 < Sc < 1339$ and $3.75 \cdot 10^{-4} < Re \cdot Fr < 6.86 \cdot 10^{-3}$, the present mass transfer data for Cd^{2+} fit the equation:

$$J_D = 0.125\ (Re \cdot Fr)^{-0.25} \tag{9}$$

with an average deviation 2.5 %.

It is worth mentioning that % removal efficiency of 99.98 (i.e. almost complete removal) was obtained for Cd^{2+}, Ni^{2+} at equilibrium, as illustrated in Fig. 10. It seems that the ion exchange resin macro-porous monoplus SP112 has high selectivity towards Cd^{2+} than Ni^{2+} as a higher % removal efficiency of Cd^{2+} than Ni^{2+} was obtained at the same time before equilibrium.

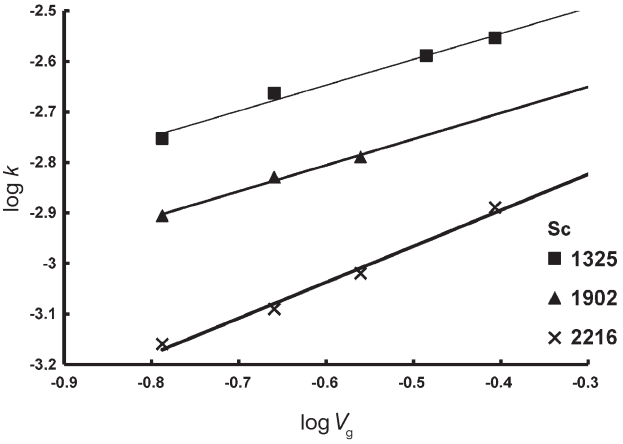

Fig. 4 – *Plot of log k vs. log v_g at different Sc for the ion exchange of Ni^{2+}. (Initial Ni^{2+} concentration = 0.05 kg m^{-3}, resin mass, m = 0.02 kg, T = 298 K).*

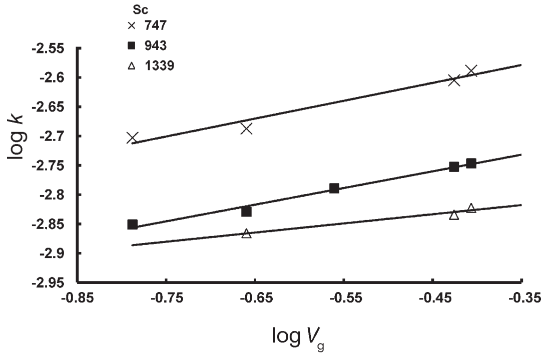

Fig. 5 – *Plot of log k vs. log v_g at different Sc for the ion exchange of Cd^{2+}. (Initial Cd^{2+} concentration = 0.05 kg m^{-3}, resin mass, m = 0.02 kg, T = 298 K).*

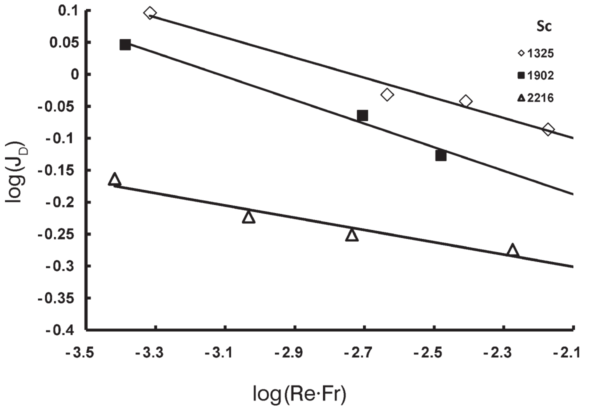

Fig. 6 – *Plot of log J_D vs. log (Re · Fr) at different Sc for the ion exchange of Ni^{2+}*

Pehlivan *et al.*[25] have found that the selectivity of $–SO_3H$ group of the strong cation resin increases with increasing atomic number, valance,

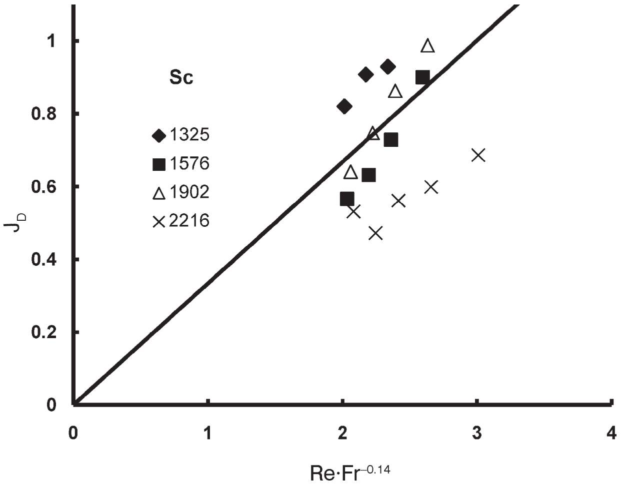

Fig. 7 – *Overall mass transfer correlation for the ion exchange of Ni^{2+}*

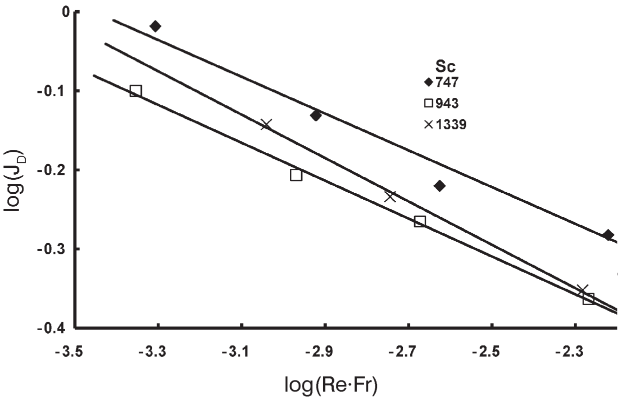

Fig. 8 – *Plot of log J_D vs. log (Re · Fr) at different Sc for the ion exchange of Cd^{2+}*

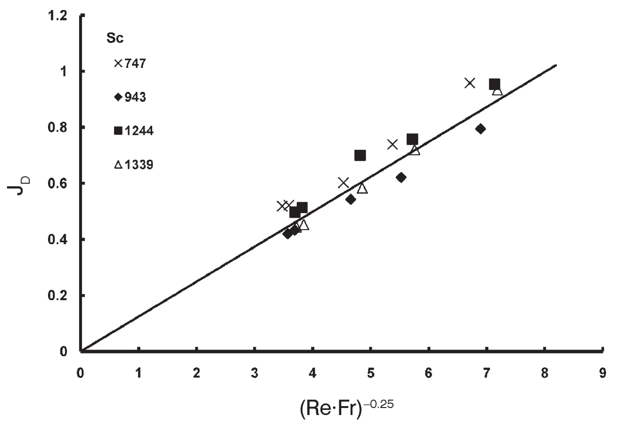

Fig. 9 – *Overall mass transfer correlation for the ion exchange of Cd^{2+}*

and degree of ionization of the exchanged metals. They also found that the selectivity of Dowex 50W, a strong cation resin, is higher towards Cd^{2+} than Ni^{2+}.

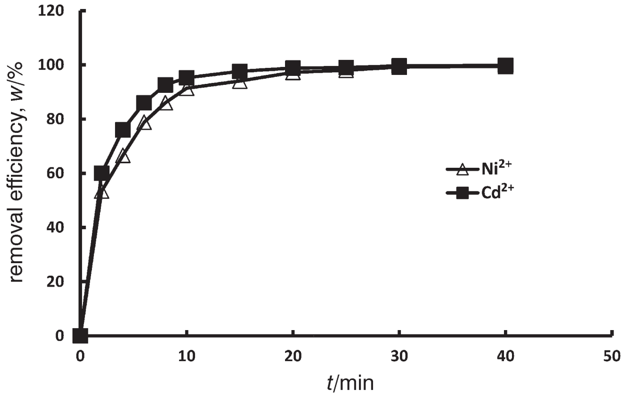

Fig. 10 – *% removal efficiency vs. time (Initial Ni^{2+} concentration = 0.05 kg m^{-3}, resin mass, m = 0.02 kg, v_g = 0.00163 m s^{-1}, T = 298 K, Initial Cd^{2+} concentration = 0.05 kg m^{-3}, resin mass, m = 0.02 kg, v_g = 0.00392 m s^{-1}, T = 298 K).*

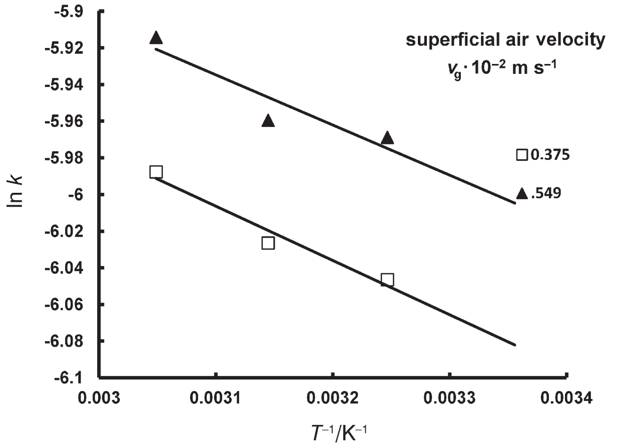

Fig. 11 – *Arrhenius plot for the ion exchange of Ni^{2+} at different superficial air velocity*

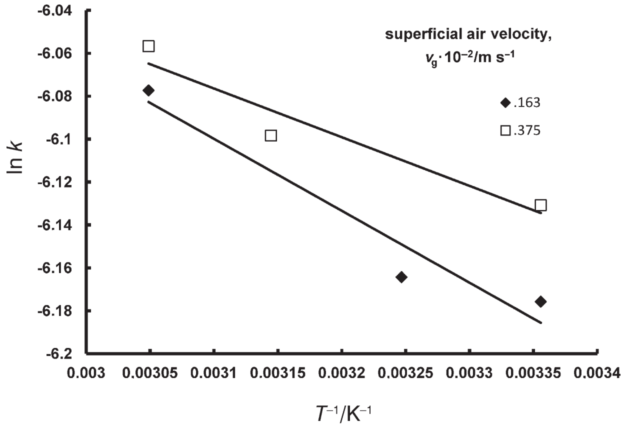

Fig. 12 – *Arrhenius plot for the ion exchange of Cd^{2+} at different superficial air velocity*

Figs. 11 and 12 show that mass transfer coefficient increases as temperature increases according to an Arrhenius equation with an average activation energy of E = 2.4 and 3.3 kJ mol^{-1} for Ni^{2+}, Cd^{2+}

respectively. These obtained values of activation energy confirm the diffusion controlled nature of the ion exchange reactions. The increase in the rate of mass transfer with temperature is attributed to the decrease in solution viscosity which increases the diffusivity of Ni^{2+} and Cd^{2+} according to Stock's-Einstein equation[14] ($D\mu/T$ = constant).

Conclusions

The present study shows that gas sparging is a promising tool for enhancing either external mass transfer controlled ion exchange reactions or mixed (external and intra-particle) controlled ion exchange reactions.

The present mass transfer data were correlated in terms of J_D, Re and Fr. These obtained mass transfer correlations can be used in practice to predict rates of mass transfer in batch gas sparged ion exchange vessels or continuous gas sparged vessels of low solution flow rate.

Temperature was found to increase the mass transfer coefficient according to an Arrhenius equation with activation energy values of $E = 2.4$ and 3.3 kJ mol^{-1} for Ni^{2+}, Cd^{2+} respectively. These values of activation energy indicate the diffusion controlled nature of the ion exchange reaction.

A maximum removal efficiency of 99.98 % has been obtained for both metal ions.

Further studies will be conducted to study a comparison between the effect of mechanical stirring and gas sparged on the rate of ion exchange reactions.

List of symbols

A – surface area of resin, m^2
a – constant
γ_0 – initial metal mass concentration, kg m^{-3}
γ – final metal mass concentration, kg m^{-3}
c – constant
D – diffusion coefficient, m^2 s^{-1}
$\bar{d}_p$ – average bubble diameter, m
$\bar{d}_s$ – average resin particle diameter, m
E – activation energy, kJ mol^{-1}
k – mass transfer coefficient, m s^{-1}
m – mass of resin, kg
n – constant
T – temperature of solution, K
t – time, s
V_s – solution volume, m^3
V_g – superficial air velocity, m s^{-1}

Greek symbol

ρ – solution density, kg m^{-3}
ρ_s – resin density, kg m^{-3}
μ – solution viscosity, kg m^{-1} s^{-1}
ν – kinematic viscosity, m^2 s^{-1}
ε – gas holdup

Dimensionless group

Fr – Froude number, $v_g{}^2/g\ d_p$
Ga – Galileo number, $g\ L^3/\nu^3$
J_D – J-factor for mass transfer, $(k/v_g)\ Sc^{0.66}$
Re – Reynolds number based on gas velocity, $\rho\ d_p\ V_g/\mu$
Sc – Schmidt number, $\mu/\rho D$
Sh – Sherwood number, $k\ d_p/D$
St – Stanton number, k/V_g

References

1. *Mubarak, A. A.,* Chem. Biochem. Eng. Q. **20** (1) (2006) 79.
2. *Mubarak, A. A., Elshazly, A. H., Konsowa, A. H.,* Desalin. **167** (2004) 127.
3. *Letord, M. M., Quemere, Coeuret, F.,* J. Electrochem. Soc. **135** (12) (1988) 3063.
4. *Ralph, T. R., Hitchman, M. L., Millington, J. P., Walsh, F. C.,* Electrochim. Acta **41** (4) (1996) 591.
5. *Fischl, D. S., Hanson, K. J., Muller, R. H., Tobias, C. W.,* Chem. Eng. Commun. **38** (1984) 191.
6. *Sara, O. N., Erkmen, J., Yapici, S., Copur, M.,* Int. Commun. Heat Mass Transfer **35** (2008) 289.
7. *Sedahmed, G. H., Abdo, M. S., Hassan, M. S., Konsowa, A. H.,* Chem. Eng. Process. **46** (2007) 10.
8. *Konsowa, A. H., Abdo, M. S., Hassan, M. S., Sedahmed, G. H.*, Chem. Eng. J. **102** (2004) 131.
9. *Nosier, S. A., Sallam, S. A.,* J. Sep. Puri. Technol. **18** (2000) 93.
10. *Sedahmed, G. H., Abdo, M. S., Kamal, M. A., Fadaly, O. A., Osman, H. M.*, Chem. Eng. Process. **40** (2001) 195.
11. *Gendron, A. S., Ettel, V.,* Can. J. Chem. Eng. **53** (1975) 36.
12. *Schweitzer, A. S., Philip, A.,* Handbook of Separation Techniques for Chemical Engineers, 2nd Edition, John Wiley and sons, New York, 1980.
13. *Nachod, S., Frederich, C.,* Ion Exchange Theory and Application, Academic Press, New York, 1949.
14. *Elshazly, A. H., Konsowa, A. H.,* J. Desalin. **158** (2003) 189.
15. *Lee, I.-H., Kuan, Y.-C., Chern, J. M.,* J. Chin. Inst. Chem. Engineers **38** (2007) 71.
16. *Coppola, L., Cavatorta, O. N., Bohm, U.,* J. Appl. Electrochem. **19** (1989) 100.
17. *Ibl, N.*, Electrochem. Acta **24** (1979) 1105.

18. *Sedahmed, G. H.,* J. Appl. Electrochem. **15** (1985) 777.
19. *Sedahmed, G. H.,* J. Appl. Electrochem. **14** (1984) 693.
20. *Glasstone, S.,* Textbook of Physical Chemistry, Macmillan, India, 1991.
21. *Cussler, E. L.,* Diffusion Mass Transfer in Fluid Systems, Cambridge press, UK, 1997.
22. *Amin, N. K., El-Ashtoukhy, E.-S. Z., Abdelwahab, O.,* Hydrometal. **224** (2007) 232.
23. *Cotton, F. A., Wilkinson, G.,* Advanced Inorganic Chemistry, Wiley Eeastern Ltd, New Deldi, 1984.
24. *Kast, W.,* Int. J. Heat Mass Transfer **5** (1962) 329.
25. *Pehlivan, E., Altun, T. J.,* Hazard. Mater. **B134** (2006) 149.